HHS Public Access

Author manuscript

Epilepsia. Author manuscript; available in PMC 2024 October 01.

Published in final edited form as:

Epilepsia. 2023 October ; 64(10): e214–e221. doi:10.1111/epi.17731.

Patient-derived *SLC6A1* variant S295L results in an epileptic phenotype similar to haploinsufficient mice

Britta E. Lindquist, MD PhD[1,2], **Yuliya Voskobiynyk, PhD**[1,2], **Kimberly Goodspeed, MD**[3], **Jeanne T. Paz, PhD**[1,2,4]

[1]Gladstone Institute of Neurological Disease, Gladstone Institutes, San Francisco, CA, 94158 USA

[2]University of California, San Francisco, Department of Neurology, Weill Institute, San Francisco, CA 94143 USA

[3]University of Texas Southwestern Medical Center, Dallas, TX 75390 USA

[4]Kavli Institute for Fundamental Neuroscience, University of California, San Francisco, San Francisco, CA 94158 USA

Abstract

The solute carrier family 6 member 1 (*SLC6A1)* gene encodes GAT-1, a GABA transporter expressed on astrocytes and inhibitory neurons. Mutations in *SLC6A1* are associated with epilepsy and developmental disorders, including motor and social impairments, but variant-specific animal models are needed to elucidate mechanisms. Here, we report electroencephalographic (ECoG) recordings and clinical data from a patient with a variant in *SLC6A1* which encodes GAT-1 with a serine-to-leucine substitution at amino acid 295 (S295L), who was diagnosed with childhood absence epilepsy. Next, we show that mice bearing the S295L mutation (GAT-$1^{S295L/+}$) have spike-and-wave discharges with motor arrest consistent with absence-type seizures, similar to GAT-$1^{+/-}$ mice. GAT-$1^{S295L/+}$ and GAT-$1^{+/-}$ mice follow the same pattern of pharmacosensitivity, being bidirectionally modulated by ethosuximide (200 mg/kg, i.p.) and the GAT-1 antagonist NO-711 (10 mg/kg, i.p.). By contrast, GAT-$1^{-/-}$ mice were insensitive to both ethosuximide and NO-711 at the doses tested. In conclusion, ECoG findings in GAT-$1^{S295L/+}$ mice phenocopy GAT-1 haploinsufficiency and provide a useful preclinical model for drug screening and gene therapy investigations.

Keywords

SLC6A1 ; absence epilepsy; spike-and-wave discharges; pharmacosensitivity; chronic wireless telemetry

Corresponding author: Name: Jeanne T. Paz, PhD, jeanne.paz@gladstone.ucsf.edu.

Conflicts of interest: None of the authors has any conflict of interest to disclose.

Ethical statement: We confirm that we have read the Journal's position on issues involved in ethical publication and affirm that this report is consistent with those guidelines. All human data collection procedures were reviewed and approved by the institutional review board of the University of Texas Southwestern Medical Center. All animal experimental procedures were reviewed and approved by the Institutional Animal Care and Use Committee at the University of California, San Francisco and Gladstone Institutes.

INTRODUCTION

The solute carrier family 6 member 1 gene (*SLC6A1*) encodes a sodium- and chloride-dependent GABA transporter, GAT-1 (1). Work in rodents has established that GAT-1 is located on astrocytes and GABAergic presynaptic terminals and modulates inhibitory neurotransmission (2, 3).

Genetic testing has identified pathogenic variants in *SLC6A1* in patients with epilepsy with myoclonic atonic seizures, absence seizures, sleep disturbances, attention deficit hyperactivity disorder, motor deficits, developmental delay, and autism, collectively referred to as *SLC6A1*-related disorders (1, 4). Mechanisms underlying different epileptic phenotypes remain poorly understood, and may depend on the specific *SLC6A1* mutation, most of which are missense mutations (5). Thus, variant-specific preclinical models are needed to accelerate the development of personalized treatments.

A mouse model of *SLC6A1*-related disorder has recently been generated by introducing a S295L missense mutation first identified in a child with developmental delay and hypotonia (4), and who later developed absence epilepsy (6). Cultured neurons and astrocytes differentiated from patient-derived induced pluripotent stem cells with this mutation show reduced GABA uptake, reduced surface expression of GAT-1, and accumulation of the mutant protein in the endoplasmic reticulum (5, 7), suggesting loss of function. Seizures have been reported in the S295L mouse (7), but the epilepsy phenotype has not been extensively characterized.

Here, we employ chronic (8 days over 2 weeks) video and wireless electrocorticographic (ECoG) recordings in freely behaving mice to characterize the epilepsy phenotype and its pharmacosensitivity in S295L mice across circadian periods and contextualize our findings with respect to partial or total loss of function in GAT-1 knock-out mice and wild-type littermate controls.

MATERIALS AND METHODS

Clinical data collection and analysis

We report interval updates in the clinical characteristics of an individual with *SLC6A1*-related disorder due to the S295L variant (4, 6). We reviewed lifetime medical records and data collected through a prospective natural history study of *SLC6A1*-related disorder. Informed consent was obtained from the legal guardian of this participant and the study was approved by the institutional review board of the study site, the University of Texas Southwestern Medical Center.

Animals

Animal protocols were approved by the Institutional Animal Care and Use Committee at the University of California, San Francisco and Gladstone Institutes. We conformed to ARRIVE guidelines (8) and recommendations to facilitate transparent reporting (9).

GAT-1 S295L (C57BL/6-*Slc6a1*$^{em2(S295L)Smoc}$; see Supplemental Methods) and GAT-1 knock-out (B6.129S1-*Slc6a1*^{tm1Lst}/Mmucd, RRID:MMRRC_000426-UCD) mouse colonies were housed in a pathogen-free barrier facility on a standard 12-hour light/dark cycle with *ad libitum* food and water. Littermate controls of both sexes were used in each experiment. Tail snips were genotyped at weaning and after euthanasia (Transnetyx genotyping services). The number of mice used in each experiment is indicated in figure legends; sex is denoted by open circles (females) and closed circles (males) in each figure.

Surgeries

Forty-nine adult mice (23 male, 26 female, 15.8 ± 0.3 weeks, 23.44 ± 0.51 g) were anesthetized (isoflurane 1–2%, 2 L/min O_2) for surgical implantation of wireless physiology transmitter devices (HD-X02, Data Sciences International, St. Paul, MN) for chronic ECoG and electromyogram (EMG) recordings, and measurement of locomotor activity; 43 mice survived to contribute data to the study. Exclusion criteria are described in Supplemental Methods.

Experimental Timeline and Pharmacosensitivity

Mice recovered for 5–7 days following surgery. Then, we activated transmitters at 7a.m. (lights on) to record baseline physiologic signals for 48 hours, in parallel with nest-building assessments (Supplemental Methods). Next, we administered pharmacologic challenges using a vehicle-controlled cross-over design (Supplemental Figure 2). All mice first received vehicle injections (normal saline 0.1 mL/10 g body weight). Next, half the animals received selective GAT-1 antagonist NO-711 (10) (Sigma N142, 10 mg/kg i.p.), then ethosuximide (Sigma E7138, 200 mg/kg i.p.). The other half of the animals first received ethosuximide, then NO-711. Drug sequence was assigned by block randomization; the experimenter was not blinded. Each drug was administered twice daily at 7a.m. (lights on) and 7p.m. (lights off) for 2 days. We ensured a ≥ 48-hour wash-out period between each drug exposure.

Detection of epileptic spikes and spike-and-wave discharges in ECoG

Digitized signals were sampled at 500 Hz (Ponemah software, SCR_017107). We removed direct current drift (0.2 s time constant) and then normalized ECoG features to baseline ECoG power, defined by root mean square (RMS) amplitude sampled during a spike-free awake interval from each animal. We detected spikes as negative-going deflections exceeding 7x RMS amplitude. We identified SWDs visually in each animal, then quantified them with a semi-automated algorithm (see Supplemental Methods).

Statistical analyses

We report values as mean ± standard error of the mean unless stated otherwise. We evaluated each data set for normality, then applied parametric or non-parametric tests as appropriate. Data analysis was performed with GraphPad Prism 7/8 (SCR_002798) and Spike2 (SCR_000903). $\alpha = 0.05$ defined the threshold for statistical significance.

RESULTS

Interictal electroencephalographic phenotype in human patient bearing the S295L variant

The index patient bearing the S295L variant initially presented at 4 to 6 months of age with global developmental delay. He sat independently at 9 months, walked at 2 years, and produced his first words by 3 years. His language regressed 3 months after onset of speech and he subsequently recovered language approximately 6 to 12 months later. At 4 years and 6 months, he was speaking in simple-phrased speech (previously reported by Kalvakuntla and colleagues (6)). Episodes of staring began in infancy; however, electroencephalograms (EEGs) obtained prior to the age of 2 years were normal. At the age of 18 months, he had spells of behavioral arrest for several seconds at a frequency of 15 per hour that resolved after a short course of oral steroids. At 2 years old, he had onset of drop spells and emergence of occipital intermittent rhythmic delta activity (OIRDA) and frontal intermittent rhythmic delta activity (FIRDA) on EEG. He was enrolled in an open-label clinical trial of phenylbutyrate in *SLC6A1*-related disorder (NCT04937062) and demonstrated resolution of staring and drop spells in addition to evolution of rhythmic delta to intermittent polymorphic delta slowing. Here, we show traces from the patient's EEG with OIRDA (which is associated with absence epilepsy (11)) and FIRDA at age 4 (Figure 1A-B). Absence epilepsy was diagnosed clinically on the basis of behavioral episodes and treatment response (6).

GAT-1 S295L variant confers an epileptic phenotype in mice

To evaluate whether mice carrying the patient-derived GAT-$1^{S295L/+}$ mutation had findings consistent with epilepsy, we obtained chronic wireless physiologic recordings from GAT-$1^{S295L/+}$ mice and wild-type littermate controls. We obtained simultaneous signals from both skeletal muscle (EMG) and brain (ECoG) in order to detect behavioral arrest during seizures using 2-channel battery-powered implantable amplifiers.

Throughout baseline recordings, GAT-$1^{S295L/+}$ mice had abundant 8-Hz SWDs associated with motor arrest indicated by reduced EMG activity (Figure 1C-D). Manual page-by-page ECoG review from GAT-$1^{S295L/+}$ mice (encompassing 336 mouse-hours) revealed no generalized tonic-clonic seizures, and none occurred during routine handling, failing to corroborate a recent report (7). SWDs appeared in both diurnal and nocturnal periods (Figure 1E-F). Interictal background ECoG otherwise resembled that of littermate controls: power, assessed by RMS amplitude during an SWD-free interval of quiet wakefulness, was similar in GAT-$1^{S295L/+}$ and GAT-$1^{+/+}$ mice (55 ± 3 vs. 53 ± 3 μV, $p = 0.62$). Male and female GAT-$1^{S295L/+}$ mice had comparable burdens of spikes (light period $p = 0.66$; dark period $p = 0.48$; n=3,4; unpaired t-tests) and SWDs (light period $p = 0.10$; dark period $p = 0.08$; n = 3,4; unpaired t-tests). Circadian patterns of locomotor activity were preserved (Figure 1G), and GAT-$1^{S295L/+}$ mice constructed nests indistinguishable from those of GAT-$1^{+/+}$ littermates (Figure 1H). We repeated the nesting assessment in a large cohort of non-implanted mice, again finding no difference in nest quality between genotypes in aggregate (GAT-$1^{+/+}$ 4.38 ± 0.12, GAT-$1^{+/S295L}$ 4.54 ± 0.14, n = 24, 23, unpaired t-test $p = 0.35$) or by sex (males $p = 0.86$; females $p = 0.30$).

We suspected that the SWDs with behavioral arrest that we observed could represent absence seizures. To better evaluate this possibility, we treated mice with intraperitoneal administration of ethosuximide (200 mg/kg), a first-line drug against absence seizure with effects on T-type Ca^{2+} channels (12) and persistent Na^{+} current (13). Ethosuximide eliminated SWDs in GAT-$1^{S295L/+}$ mice for approximately one hour following each administration (Figure 1I-K). Conversely, intraperitoneal administration of NO-711 (10 mg/kg) acutely provoked SWDs in wild-type GAT-$1^{+/+}$ mice and dramatically increased the number of SWDs in GAT-$1^{S295L/+}$ mice, inducing nearly continuous SWDs and immobility (Figure 1L-M) for up to four hours. We employed spike detection to quantify long episodes under-detected by our SWD algorithm. Drug effects on epileptic activity were robust in both light and dark periods (Figure 1I-M).

Gradient of epileptic abnormalities with progressive GAT-1 deficiency

Gene dose-dependence of the epilepsy resulting from GAT-1 loss of function has not, to our knowledge, been previously described: prior reports have evaluated ECoG in homozygous GAT-$1^{-/-}$ but not heterozygous GAT-$1^{+/-}$ mice (14). To address this gap, we obtained chronic wireless ECoG and EMG recordings from mice lacking 0, 1, or 2 copies of the *Slc6a1* gene, corresponding to 100%, ~ 65%, and < 2% rates of GAT-1 mediated [^{3}H]GABA uptake, respectively (15).

We observed a gradient of epileptic abnormalities with progressive GAT-1 deficiency. Wildtype GAT-$1^{+/+}$ mice had normal ECoG, whereas GAT-$1^{+/-}$ mice had frequent SWDs associated with motor arrest (Figure 2A). Similar seizure frequencies were observed in heterozygous GAT-$1^{+/-}$ mice vs. GAT-$1^{S295L/+}$ knock-in animals (Supplemental Figure 3). GAT-$1^{-/-}$ mice exhibited severe ECoG abnormalities with long episodes of continuous slow (6-Hz) spike-and-wave activity corresponding to prolonged periods of immobility (Figure 2A-B). The baseline RMS amplitude of background ECoG, sampled from a spike-free interval of quiet wakefulness, was increased in GAT-$1^{-/-}$ mice compared with littermates (83 ± 3 vs. 52 ± 2 vs. 53 ± 2 μV, n = 9,9,9, $p < 0.0001$ ANOVA; $p < 0.0001$ Tukey's multiple comparisons test). Despite grossly abnormal ECoG and frequent SWDs with motor arrest, both diurnal and nocturnal periods (Figure 2C-D), circadian patterns of activity were preserved in mice with GAT-1 loss of function (Figure 2E). Males and females had similar ECoG abnormalities (spike frequency male vs female GAT-$1^{+/-}$ day p = 0.78, night 0.80; GAT-$1^{-/-}$ day $p = 0.83$, night $p = 0.83$, n = 5,4; unpaired t-tests). GAT-$1^{-/-}$ mice constructed poor-quality nests compared with GAT-$1^{+/+}$ and GAT-$1^{+/-}$ littermates (Figure 2F); this effect appeared to be driven by males (male GAT-$1^{+/+}$ vs. GAT-$1^{+/-}$ vs. GAT-$1^{-/-}$ ANOVA $p = 0.0098$, n = 4,5,4; Dunnett's multiple comparisons $p = 0.32$ GAT-$1^{+/+}$ vs. GAT-$1^{+/-}$, $p = 0.006$ GAT-$1^{+/+}$ vs. GAT-$1^{-/-}$) and did not reach significance in females (female GAT-$1^{+/+}$ vs. GAT-$1^{+/-}$ vs. GAT-$1^{-/-}$ ANOVA $p = 0.19$, n = 4,3,4).

Ethosuximide (200 mg/kg) transiently eliminated SWDs in GAT-$1^{+/-}$ mice (Figure 2G-H). The severe phenotype in GAT-$1^{-/-}$ mice was resistant to ethosuximide in our hands at the dose and time-point tested (Figure 2J).

In GAT-$1^{+/-}$ and GAT-$1^{+/+}$ mice, systemic NO-711 (10 mg/kg) administration provoked continuous SWDs (Figure 2G-H), similar to a prior report of SWDs induced by

intrathalamic NO-711 infusion in Wistar rats (14). By contrast, NO-711 had no effect on GAT-1$^{-/-}$ mice lacking surface expression of the drug target (Figure 2G-H). Indeed, GAT-1$^{-/-}$ mice ambulated intermittently during the hour following NO-711 administration, whereas the same dose rendered wild-type littermates immobile (Figure 2I-J, $p = 0.0009$ (light period); $p < 0.0001$ (dark period), n = 8,9, Welch's t-tests with Bonferroni correction).

In summary, ethosuximide-sensitive SWDs were abundant in GAT-1$^{S295L/+}$ and GAT-1$^{+/-}$ mice and exacerbated by NO-711. A more severe pharmacoresistant epilepsy phenotype with nesting impairment was seen in homozygous GAT-1$^{-/-}$ mice.

CONCLUSIONS

We provide a clinical update including EEG traces from a patient carrying a variant in *SLC6A1*, encoding a missense mutation (S295L) in GABA transporter GAT-1, who has absence epilepsy. Using chronic wireless telemetry, we found that mice carrying the same point mutation exhibited ethosuximide-sensitive SWDs with motor arrest, consistent with absence seizures. The epilepsy in GAT-1$^{S295L/+}$ mice resembled that of GAT-1$^{+/-}$ mice in quality and severity, and both were exacerbated by GAT-1 antagonist NO-711, indicating the presence of significant surface expression of functional protein and arguing against a dominant negative mechanism of action. There was a progressive dose-response relationship between the degree of *Slc6a1* ablation and the severity of the resulting epilepsy phenotype, with prolonged SWDs and immobility associated with impaired nesting behavior in GAT-1$^{-/-}$ mice.

Our results are consistent with the proposition that GAT-1 S295L is a loss-of-function mutation that confers disease by a mechanism of haploinsufficiency, consistent with *in vitro* functional assays (5). Our findings are broadly relevant to other *SLC6A1* mutations because most are characterized by loss of function (5, 16-18). Moreover, these results strongly support the therapeutic potential of chemical chaperones that rescue GAT-1 trafficking deficits associated with S295L (7), and perhaps other variants.

How a loss of function in the GAT-1 transporter results in epilepsy in *SLC6A1*-related disorders remains incompletely understood. A possibility suggested by previously published work in knockout mice is that reduced GABA uptake by thalamic astrocytes results in enhanced tonic GABA current mediated by activation of extrasynaptic $GABA_A$ receptors in thalamic neurons. In turn, enhanced tonic GABA current hyperpolarizes thalamocortical neurons and paradoxically increases their firing by facilitating post-inhibitory rebound bursts of action potentials, which results in SWDs (3, 14, 19, 20). Whether these mechanisms are responsible for epileptic findings in S295L mice remains to be determined.

We acknowledge that animal studies are imperfect in modeling human disease. Many variants cause different phenotypes in humans than in mice, which have less complex brain circuitry, express a relatively impoverished repertoire of cognitive behaviors and epileptic seizure types, and cannot report subjective symptoms. Another limitation of the present study is that we recorded unilateral (rather than bilateral) ECoG, a trade-off of the 2-channel battery-powered implantable wireless amplifiers we selected, and our choice to

monitor EMG as a time-locked behavioral read-out; thus, we cannot confidently assert that SWDs were generalized. The fact that the S295L mouse displays SWDs with behavioral arrest is consistent with the diagnosis of absence epilepsy in the index patient (6). Our findings provide additional supportive evidence that S295L is a pathogenic variant, and the GAT-1$^{S295L/+}$ mouse is a promising model for future mechanistic and translational studies.

Supplementary Material

Refer to Web version on PubMed Central for supplementary material.

ACKNOWLEDGEMENTS

Research funding was provided by SLC6A1 Connect, Taysha Gene Therapies, and Gladstone Institutes, with salary support from Gladstone Institutes, NIH NINDS R01NS096369 and DoD EP150038 (JTP), Berkelhammer Postdoctoral Fellowship, CIRM Scholarship, and NIH/NINDS 1F32NS127998-01 (YV), and NIH NINDS R25 NS070680 to UCSF (BEL). We thank Frances S. Cho for technical assistance with surgeries and Deanna Necula for technical assistance with data visualization. We thank Irene Lew and Zanib Naeem for assistance with animal husbandry. We thank Dan Feng of Shanghai Model Organisms for procuring GAT-1$^{S295L/+}$ mice. We thank Henry Lester at the California Institute of Technology for donating GAT-1$^{S295L/+}$ mice to the Mutant Mouse Resource & Research Centers supported by NIH (MMRC). We thank Steven Gray at the University of Texas Southwestern Medical Center for sharing GAT-1$^{-/-}$ mice. We also thank Clare Timbie, Francoise Chanut, and Deanna Necula for critical feedback on our manuscript.

Funding:

BEL is supported by NIH/NINDS R25 fellowship to UCSF (R25NS070680). JTP is supported by NIH/NINDS grant R01NS096369, Gladstone Institutes, and the DoD (EP150038). YV is supported by NIH/NINDS 1F32NS127998-01. This project was also funded by Gladstone Institutes, SLC6A1 Connect, and Taysha Gene Therapies. KG is supported by SLC6A1 Connect and the University of Texas Southwestern Dedman Family Scholar in Clinical Care endowment.

Data availability:

The data supporting this study's findings are available from the corresponding author upon reasonable request.

REFERENCES

1. Goodspeed K, Demarest S, Johannesen K, Kang J, Lal D, Angione K. SLC6A1-Related Neurodevelopmental Disorder. In: Adam MP, Mirzaa GM, Pagon RA, Wallace SE, Bean LJH, Gripp KW, et al., editors. GeneReviews((R)). Seattle (WA)2023.
2. Chiu CS, Jensen K, Sokolova I, Wang D, Li M, Deshpande P, et al. Number, density, and surface/cytoplasmic distribution of GABA transporters at presynaptic structures of knock-in mice carrying GABA transporter subtype 1-green fluorescent protein fusions. J Neurosci. 2002;22(23):10251–66. [PubMed: 12451126]
3. Pirttimaki T, Parri HR, Crunelli V. Astrocytic GABA transporter GAT-1 dysfunction in experimental absence seizures. J Physiol. 2013;591(4):823–33. [PubMed: 23090943]
4. Goodspeed K, Perez-Palma E, Iqbal S, Cooper D, Scimemi A, Johannesen KM, et al. Current knowledge of SLC6A1-related neurodevelopmental disorders. Brain Commun. 2020;2(2):fcaa170. [PubMed: 33241211]
5. Mermer F, Poliquin S, Rigsby K, Rastogi A, Shen W, Romero-Morales A, et al. Common molecular mechanisms of SLC6A1 variant-mediated neurodevelopmental disorders in astrocytes and neurons. Brain. 2021;144(8):2499–512. [PubMed: 34028503]

6. Kalvakuntla S, Lee M, Chung WK, Demarest S, Freed A, Horning KJ, et al. Patterns of developmental regression and associated clinical characteristics in SLC6A1-related disorder. Front Neurosci. 2023;17:1024388. [PubMed: 36895422]
7. Nwosu G, Mermer F, Flamm C, Poliquin S, Shen W, Rigsby K, et al. 4-Phenylbutyrate restored gamma-aminobutyric acid uptake and reduced seizures in SLC6A1 patient variant-bearing cell and mouse models. Brain Commun. 2022;4(3):fcac144. [PubMed: 35911425]
8. Group NRRGW. Animal research: reporting in vivo experiments: the ARRIVE guidelines. J Physiol. 2010;588(Pt 14):2519–21. [PubMed: 20634180]
9. Landis SC, Amara SG, Asadullah K, Austin CP, Blumenstein R, Bradley EW, et al. A call for transparent reporting to optimize the predictive value of preclinical research. Nature. 2012;490(7419):187–91. [PubMed: 23060188]
10. Keros S, Hablitz JJ. Subtype-specific GABA transporter antagonists synergistically modulate phasic and tonic GABAA conductances in rat neocortex. J Neurophysiol. 2005;94(3):2073–85. [PubMed: 15987761]
11. Guilhoto LM, Manreza ML, Yacubian EM. Occipital intermittent rhythmic delta activity in absence epilepsy. Arq Neuropsiquiatr. 2006;64(2A):193–7. [PubMed: 16791354]
12. Coulter DA, Huguenard JR, Prince DA. Characterization of ethosuximide reduction of low-threshold calcium current in thalamic neurons. Ann Neurol. 1989;25(6):582–93. [PubMed: 2545161]
13. Leresche N, Parri HR, Erdemli G, Guyon A, Turner JP, Williams SR, et al. On the action of the anti-absence drug ethosuximide in the rat and cat thalamus. J Neurosci. 1998;18(13):4842–53. [PubMed: 9634550]
14. Cope DW, Di Giovanni G, Fyson SJ, Orban G, Errington AC, Lorincz ML, et al. Enhanced tonic GABAA inhibition in typical absence epilepsy. Nat Med. 2009;15(12):1392–8. [PubMed: 19966779]
15. Jensen K, Chiu CS, Sokolova I, Lester HA, Mody I. GABA transporter-1 (GAT1)-deficient mice: differential tonic activation of GABAA versus GABAB receptors in the hippocampus. J Neurophysiol. 2003;90(4):2690–701. [PubMed: 12815026]
16. Cai K, Wang J, Eissman J, Wang J, Nwosu G, Shen W, et al. A missense mutation in SLC6A1 associated with Lennox-Gastaut syndrome impairs GABA transporter 1 protein trafficking and function. Exp Neurol. 2019;320:112973. [PubMed: 31176687]
17. Wang J, Poliquin S, Mermer F, Eissman J, Delpire E, Wang J, et al. Endoplasmic reticulum retention and degradation of a mutation in SLC6A1 associated with epilepsy and autism. Mol Brain. 2020;13(1):76. [PubMed: 32398021]
18. Mermer F, Poliquin S, Zhou S, Wang X, Ding Y, Yin F, et al. Astrocytic GABA transporter 1 deficit in novel SLC6A1 variants mediated epilepsy: Connected from protein destabilization to seizures in mice and humans. Neurobiol Dis. 2022;172:105810. [PubMed: 35840120]
19. Cho FS, Vainchtein ID, Voskobiynyk Y, Morningstar AR, Aparicio F, Higashikubo B, et al. Enhancing GAT-3 in thalamic astrocytes promotes resilience to brain injury in rodents. Sci Transl Med. 2022;14(652):eabj4310. [PubMed: 35857628]
20. Lindquist BE, Timbie C, Voskobiynyk Y, Paz JT. Thalamocortical circuits in generalized epilepsy: Pathophysiologic mechanisms and therapeutic targets. Neurobiol Dis. 2023:106094. [PubMed: 36990364]

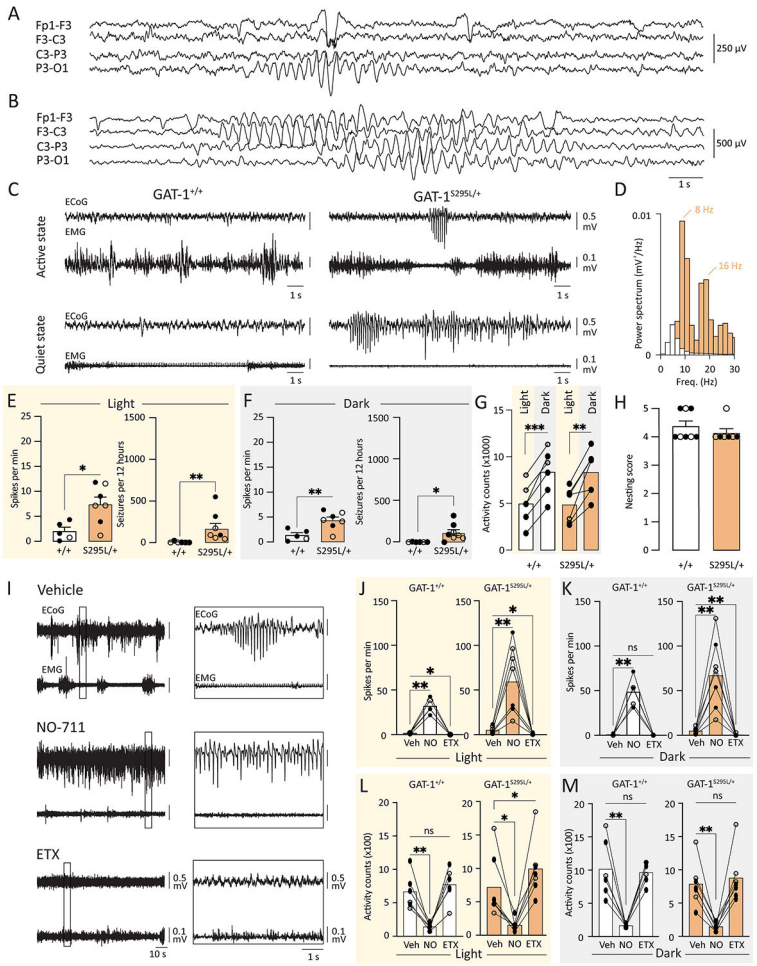

Figure 1.

Patient-derived *Slc6a1* variant S295L is associated with absence epilepsy in human and mouse. **A-B.** Scalp EEG traces from a 4-year-old boy with S295L variant *SLC6A1*-related disorder, illustrating: **A.** occipital intermittent rhythmic delta activity (dimensions proportional to sensitivity 15 µV/mm, paper speed 30 mm/s) and **B.** frontal intermittent rhythmic delta activity (sensitivity 30 µV/mm, paper speed 30 mm/s). For each, a limited montage is shown; see Supplemental Figure 3 for a standard 10–20 montage. **C.** ECoG and EMG recordings from representative wild-type and S295L variant mice during active (top traces) and quiet (bottom traces) behavioral states. **D.** Spectral density plot of ECoG, evaluated during the active segment shown in (A) in GAT-1$^{S295L/+}$ (orange) and GAT-1$^{+/+}$ (white) mice. **E.** Quantification of spikes and SWDs occurring during the light period, averaged over two consecutive 12-hour light periods (n = 5, 7, Mann-Whitney test). **F.** Quantification of spikes and SWDs occurring during the dark period (n = 5, 7, Mann-Whitney test). **G.** Circadian patterns of locomotor activity in GAT-1$^{+/+}$ (n = 6, p = 0.0002, paired t-test) and GAT-1$^{S295L/+}$ mice (n = 7, p = 0.0022, paired t-test). **H.** Nest building, scored at 48 hours on a 6-point (0–5) scale (n = 8, 7, p = 0.3457, unpaired t-test). This panel captures data from some mice without ECoG or locomotor activity (mice underwent device implantation surgery and recovery but no ECoG was recorded due to

transmitter failure). **I.** Pharmacosensitivity of epileptic phenotype in GAT-1$^{S295L/+}$ mice, demonstrated by ECoG and EMG traces from a representative GAT-1$^{S295L/+}$ mouse. See also Supplemental Figure 2. J-K. Population data summarizing ECoG changes in GAT-1$^{+/+}$ (white bars) and GAT-1$^{S295L/+}$ mice (orange bars) in response to vehicle, NO-711, and ethosuximide, assessed at 7a.m. (**I**) and at 7p.m. (**J**). RM-ANOVA with Dunnett's multiple comparisons tests, n = 5, 8. **L-M.** Population data summarizing locomotor activity changes in GAT-1$^{+/+}$ (white bars) and GAT-1$^{S295L/+}$ mice (orange bars) in response to vehicle, NO-711, and ethosuximide, assessed at 7a.m. (**L**) and at 7p.m. (**M**) Data represent the first hour post-injection. The sequence of drug administration (NO-711 vs ethosuximide) was alternated in interleaved animals to control for order effects, if any. * $p < 0.05$, ** $p < 0.01$. Each dot represents a single mouse (solid circles: males, open circles: females).

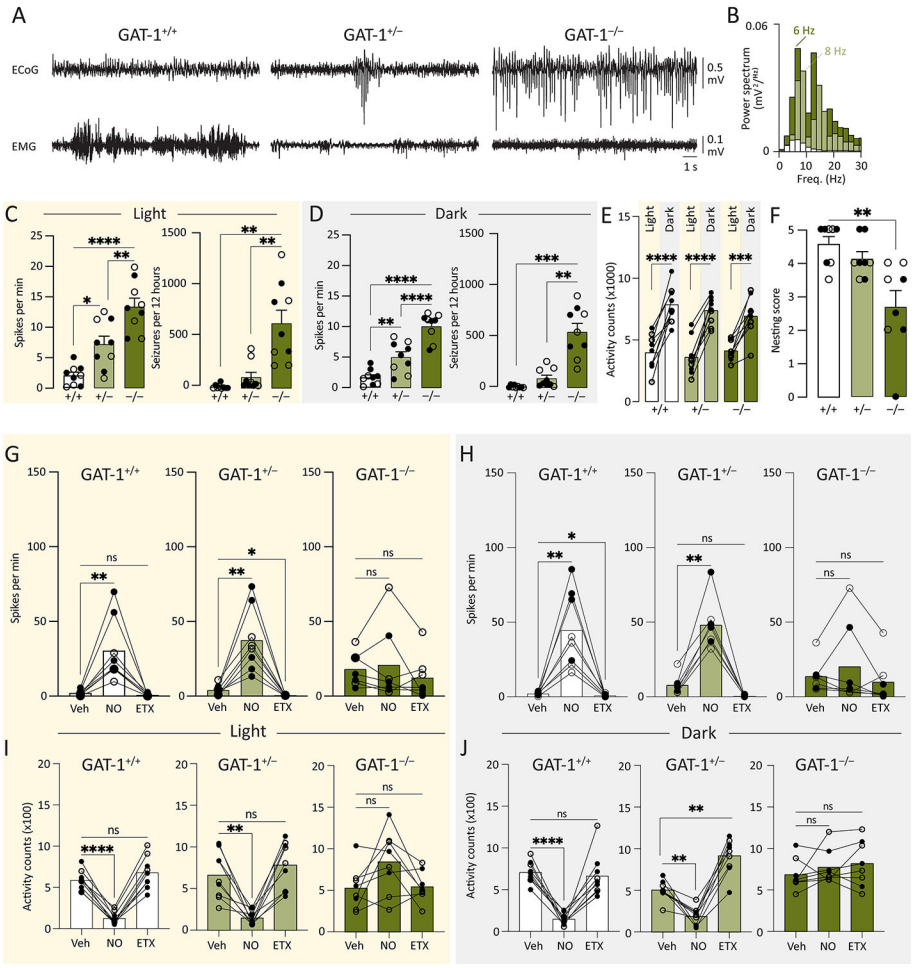

Figure 2.

Gradient of epileptic abnormalities with progressive GAT-1 deficiency. **A.** Simultaneously recorded ECoG (top) and EMG (bottom) activity from representative GAT-$1^{+/+}$ (left), GAT-$1^{+/-}$ (middle), and GAT-$1^{-/-}$ (right) mice. **B.** Spectral density plot of ECoG during the interval shown in (A) in GAT-$1^{+/+}$ (white), GAT-$1^{+/-}$ (light green), and GAT-$1^{-/-}$ (dark green) mice. **C.** Spike and SWD quantification averaged over two consecutive 12-hour light periods (spikes ANOVA $p < 0.0001$, Tukey's multiple comparisons, n = 9,9,9; SWDs Brown-Forsythe $p < 0.0005$, Dunnett's multiple comparisons, n = 9,9,9). **D.** Quantification of spikes and SWDs, averaged over two consecutive dark periods (spikes, ANOVA $p = 0.04$, Tukey's multiple comparisons, n = 9,9,9; SWDs, Brown-Forsythe $p < 0.0001$, Dunnett's multiple comparisons, n = 9,9,9). **E.** Circadian patterns of locomotor activity in the GAT-1 colony (GAT-$1^{+/+}$ $p < 0.0001$, GAT-$1^{+/-}$ $p < 0.0001$, GAT-$1^{-/-}$ $p = 0.0003$, paired t-tests, n = 9,9,9). **F.** Quantification of nesting behavior (ANOVA $p = 0.0015$; post-hoc t-tests with Dunnett's correction, n = 8,8,8). **G-J.** Pharmacosensitivity of GAT-1 knock-out mice. **G.** Population data plotting spike burden under conditions of vehicle, NO-711, and ethosuximide administration at 7a.m. (See also Supplemental Figure 2. GAT-$1^{+/+}$ RM-ANOVA $p = 0.005$, Dunnett's multiple comparison test; n = 8; GAT-$1^{+/-}$ RM-ANOVA $p = 0.002$, Dunnett's multiple comparisons; n = 8; GAT-$1^{-/-}$ RM-ANOVA $p = 0.37$, n

= 8). **H.** Population data plotting spike burden under conditions of vehicle, NO-711, and ethosuximide administration at 7p.m. (GAT-$1^{+/+}$ RM-ANOVA $p = 0.002$, Dunnett's multiple comparisons, n = 8; GAT-$1^{+/-}$ RM-ANOVA $p = 0.0001$, Dunnett's multiple comparisons, n = 7; GAT-$1^{-/-}$ RM-ANOVA $p = 0.026$, n = 7). Data shown represent the first hour post-injection. The sequence of drug administration (NO-711 vs. ethosuximide) was alternated in interleaved animals to mitigate any order effects, similar to Fig. 1. *$p < 0.05$, **$p < 0.01$. Each dot represents a single mouse (solid circles: males, open circles: females).